Storage of Al/AlF_3 Thin-Film Mirrors in 327 K Oven

Kenan Fronk

A senior thesis submitted to the faculty of

Brigham Young University

in partial fulfillment of the requirements for the degree of

Bachelor of Science

David Allred, Advisor

Department of Physics and Astronomy

Brigham Young University

April 2021

Copyright © 2021 Kenan Fronk

All Rights Reserved

ABSTRACT

Storage of Al/AlF_3 bilayer thin films in 327 K oven

Kenan Fronk

Department of Physics and Astronomy

Bachelor of Science

NASA is preparing to send new telescopes into space with the capacity to see into the far ultraviolet (UV) spectrum. Many materials lose their reflectance the farther into the UV that they go, but Al is a prime candidate because of its good reflectance in the far ultraviolet. As such, mirrors with Al bases and protective layers are being researched as candidates for the thin film mirrors needed on future telescopes. Without a protective layer, Al oxidizes and loses much of its far-ultraviolet reflectance. Prior to sending telescopes into space, many components are placed in storage for extended periods of time. While in storage, thin films may degrade depending on the temperature or humidity of the environment. We stored multiple Al coated with 30 nm AlF_3 bilayer mirrors in a 327 K oven in dry air (276 K dew point) to simulate a hot storage room. The Al layers for all samples are 20 nm. Using spectroscopic ellipsometry over the 190 to 1700 nm range to periodically measure samples, we found that there was no significant change in the ~30 nm AlF_3 capping layer over a period of 2500 hours.

Keywords: thin films, mirrors, ultraviolet, aluminum, aluminum fluoride, storage, lifetime studies

Acknowledgements

We would like to acknowledge the BYU Department of Physics and Astronomy for funding our research efforts. We also wish to thank Dr. Matthew R. Linford for giving us access to his ellipsometer and John Ellsworth for letting us borrow the oven used in this study. I am grateful to Joshua Vawdrey who made measurements of sample roughness. Finally, I personally wish to thank the members of the Extreme Ultraviolet and Thin Films research group and my advisor Dr. David Allred.

Contents

Table of Contents iii

List of Figures iv

List of Tables v

1 **Introduction** ... 1
2 **Methods and Analysis** ... 4
2.1 **Deposition of Al and AlF_3** ... 4
2.2 **Characterization** ... 7
2.2.1 **Characterization via spectroscopic Ellipsometry** ... 7
2.2.2 **Characterization via AFM** ... 11
2.3 **Storage in 327 K Oven** ... 11
3 **Results and Discussion** ... 13
3.1 **Initial fit before layer parameter optimization** ... 13
3.2 **Difficulties with the EMA model** ... 14
3.2.1 **Water as a secondary constituent** ... 14
3.2.2 **Void as a secondary constituent** ... 15
3.3 **Final fit after layer parameter optimization** ... 16
3.4 **Root Mean Squared Error** ... 17
3.5 **Conclusion** ... 19
References ... 20
Index ... 21

List of Figures

FIG. 1. Decrease in computed reflectance over far ultraviolet wavelengths as a function of aluminum oxide growth. 2

FIG. 2. The apparatus used to deposit Al and AlF_3 on the Si/Si_3N_4 substrate wafers. 5

FIG. 3. Representation of the optical stack of the samples created. 8

FIG. 4. The initial fit and the trends of each of the samples' AlF_3 layer over the duration in the oven. 13

FIG. 5. The constituent "water" percent for the samples over time. 15

FIG. 6. Void percentage of the samples over time. 16

FIG. 7. The final fits of the AlF_3 capping layers for all four samples. 17

FIG. 8. The RMSE between the ellipsometric data and our model for each sample. 18

List of Tables

TABLE 1: The initial apparent layer thicknesses measured after deposition for each of the four samples.. 11

TABLE 2: All samples from the final data set for each sample were fit to $y = A\ln t + B$ where t is measured in hours. 17

1 Introduction

Performance of telescopes depend largely on the reflectance of the mirrors being used. Thin-film mirrors used in telescope applications need to be made from a material that provides high reflectance for both high and low energy light. Aluminum (Al) is the best candidate for a broadband high reflectance material. Theoretical calculations in Fig. 1 show that Al may be able to provide >85% reflectance up to 14 eV (>89 nm) and >90% reflectance over most of the 0-14 eV range. However, as Al oxidizes, its reflectance drops significantly. Even 1 nm of oxidation in the theoretical calculations show a significant drop in reflectance, especially as the wavelength of light decreases. Unfortunately, Al is prone to oxidation, even under high vacuum conditions. To combat oxidation a fluoride capping layer can be utilized to help seal off the Al. Metallic fluorides with high band gaps, like lithium fluoride (LiF) are ideal capping layers. However, LiF is hygroscopic and degrades in environments with water. Instead, magnesium fluoride (MgF_2) and more recently, aluminum fluoride (AlF_3) layers are being used because they are more stable and less susceptible to water than LiF [1]. In this study, we wanted to explore how, or if, the storage of AlF_3-capped Al mirrors in an environment similar to a hot summer storage room would affect the apparent thickness of the capping layer or the rate of oxidation of the capped Al.

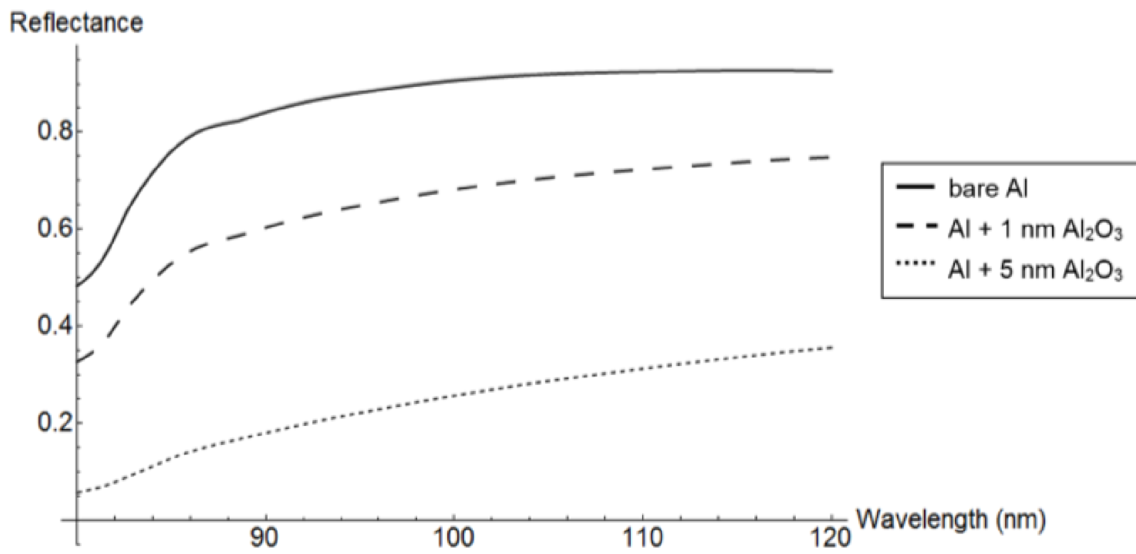

FIG. 1. Decrease in the computed reflectance over far ultraviolet wavelengths as a function of aluminum oxide thickness.

Despite the growing usage of metallic fluorides as capping layers, there remain questions as to how these protective layers change over time. High reflectance mirrors are often created and then are stored for months or years before being sent into space. During these durations, it is imperative that there is no significant swelling or shrinking in the capping layer as it can be detrimental to the intended reflectance. As such, we are interested in better understanding under what conditions these capping layers change in order to protect the intended thickness of the capping layer.

In this study we created four AlF_3-capped Al thin-film mirrors and placed them in an oven to simulate a hot storage room in summer. The samples were then periodically measured using an ellipsometer to gauge the apparent thicknesses of the Al and AlF_3 over time. Chapter 2 explains how we created the samples, how we characterized them, and in what environment we stored them. Chapter 3 outlines our results, the takeaways from this study, and what we intend to work on in the future. The results from this study will help better educate the community as whether or not the storage of AlF_3 on Al bilayer films in a 327 K environment causes significant

changes in the capping layer thickness. In this way, the thin-film mirror and telescope community will be able to better understand how temperature affects mirrors when they are in storage before use.

2 Methods and Analysis

2.1 Deposition of Al and AlF_3

Four AlF_3 on Al bilayer films were deposited on a 300 nm silicon nitride (Si_3N_4) coated Si wafer using a Veeco thermal evaporator for this study of the aging of AlF_3-protected mirror coatings. In addition, a single layer of AlF_3 on Si was prepared, measured and its aging studied. The evaporator had three independent, resistance-heated evaporation sources with two independent power supplies, so that Al and AlF_3 could be deposited immediately one after the other without breaking vacuum and with minimal time between layer depositions. The Al was evaporated from a tungsten coil and the chunks of AlF_3 were evaporated in a standard (RD Mathis) molybdenum evaporation boat.

An Inficon quartz-crystal thickness monitor (QCM) provided the feedback to control film thickness and deposition rates. An electronic oscillator drives the quartz crystal and monitors changes in its frequency as material is deposited on it, which allowed for a quick and precise way to measure deposition thickness in situ[1]. Two separate manual shutters were used in the deposition processes to control film thickness. Figure 2 shows the equipment and setup of the evaporation chamber. The top shutter was placed immediately below the substrates on the sample platen- closed, it covered the substrates so that they were out of the line-of-sight of all evaporation sources; opened, and evaporated molecules could reach the substrates from whatever sources that were hot enough and were not covered by the lower shutter. The lower shutter sat between two deposition sources: Al and AlF_3. It is flag shaped. Its rotation axis was horizontal

[1] More information on Inficion QCM crystals can be found at infinicon.com.

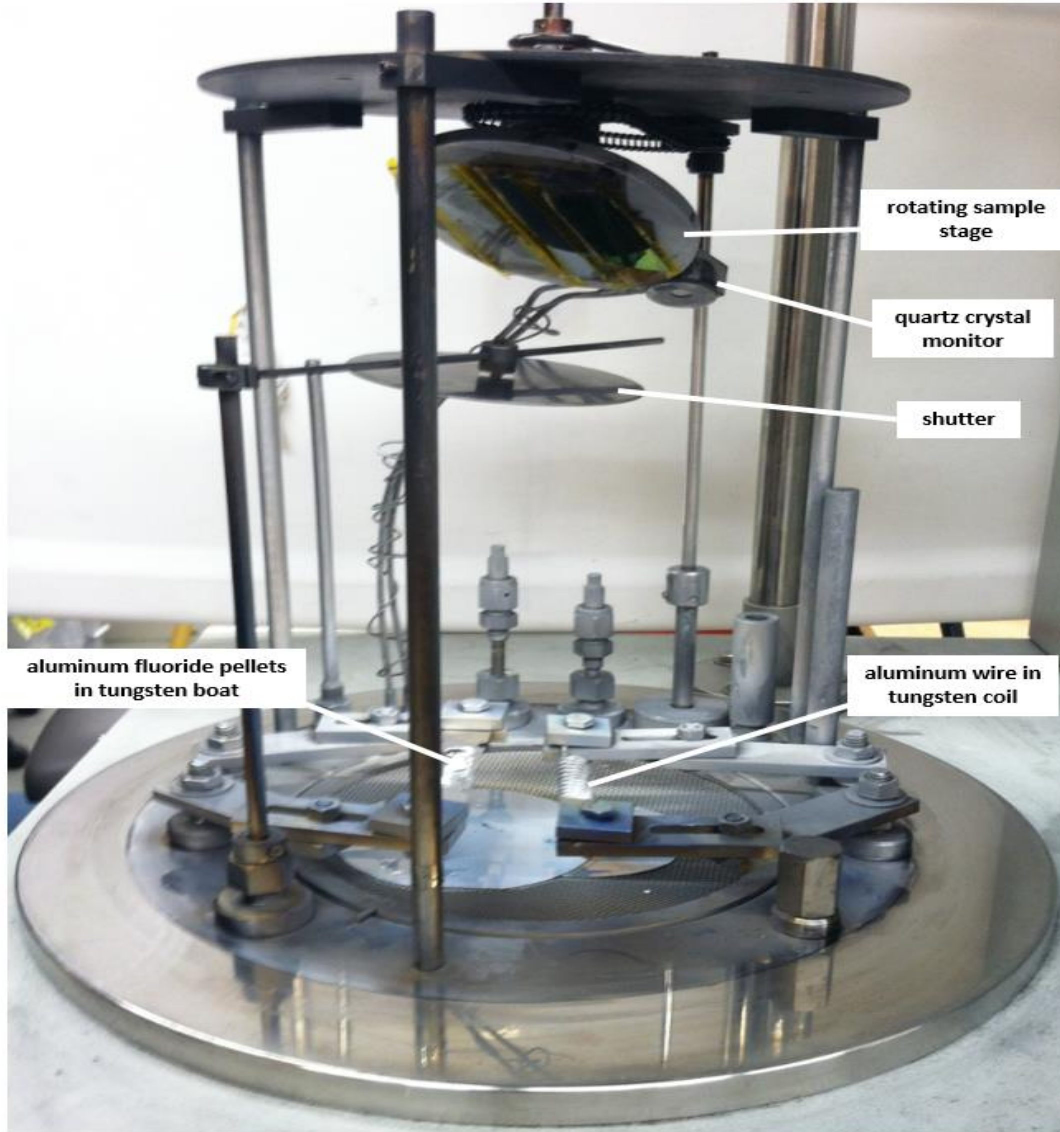

FIG. 2. The apparatus used to deposit Al and AlF_3 on the Si/Si_3N_4 substrate wafers. Note that both the Al and AlF_3 are in different boats and the shutter is used to control how much evaporated material hits the samples. Although not shown in this picture, there was an additional flag-shaped shutter between the two evaporation sources.

and lay between the two sources. The axis was attached to a rotational feedthrough. Tilting the flag to the right covered the AlF_3 source but left the Al source line-of-sight access to the chamber. Tilted sufficiently to the left, it covered the Al source, but gave the AlF_3 molecules evaporating from that source line-of-sight access to the chamber. Thus, both sources could be hot, but only one at a time would be coating the substrates, with the advantage that one could switch immediately from depositing Al to depositing AlF_3. Doing this minimized the time the

freshly evaporated Al films were left bare to a couple of seconds. This is important since even under high vacuum conditions the far ultraviolet (FUV) reflectance of a freshly evaporated Al surface begins to fall in seconds as it begins to oxidize. Turning now to the substrate holder, the 40 cm diameter sample platen was drilled like an optical breadboard with threaded holes every inch. It sat about 37 cm above the evaporation sources covering the top of the bell jar when it was in place.

It is long known that many fluorides such as MgF_2 and LiF have superior FUV optical properties when deposited at elevated temperatures [2]. Prior research shows that the optical properties of evaporated AlF_3 improve significantly when deposited on heated substrates above 200°C, so a heater was constructed, and half the samples were prepared on a heated substrate [3]. The lab-built substrate heater consisted of a pair of 12V resistance heaters in an aluminum case with rectangular dimensions of 26 mm x 60 mm placed side-by-side. The heater temperature used for the heated samples was about 510 ± 15 K.

For the AlF_3 on Al samples, approximately 30 mm by 30 mm squares were cleaved from a 200 nm diameter Si (100) wafer coated with a nominal 300 nm of chemical vapor deposited (CVD) Si_3N_4. The CVD Si_3N_4 dielectric layer on the substrate is referred to as the interference layer and is useful for detecting the oxidation of the Al if the Al layer is semitransparent. In preparing the first four samples, half of the samples were fixed directly to the 40 cm diameter sample platen, while the remainder were fixed to a heater mounted directly to the platen stage. During deposition, the heater had a nominal temperature of 473 ± 10 K. The Al was evaporated at a rate of 0.7 nm/sec and the AlF_3 was evaporated at a rate of 0.15 nm/sec. Both the Al and AlF_3 were deposited sequentially without breaking vacuum. The chamber pressure was

4×10^{-4} Pa prior to evaporation. Deposition of both Al and AlF_3 took roughly four minutes. All four samples had a 20 nm Al layer capped with a ~30 nm AlF_3 layer.

2.2 Characterization

2.2.1 Characterization via spectroscopic Ellipsometry

We measured the apparent thicknesses of the thin-film mirror samples in this study using variable-angle, spectroscopic ellipsometry. Ellipsometry is a method of measuring apparent thin-film layer thicknesses by measuring changes in polarized light as compared to a model. Linearly polarized light is reflected off the sample surface at varying angles which causes the polarization of the light to change. The reflected polarized light is then analyzed, and the subsequent data can be used to determine layer thicknesses. We chose ellipsometry as our method for tracking the thicknesses of the films because measurements can be made easily and quickly. The models used for each layer are discussed in this section.

Immediately after the initial deposition, the samples were removed from the deposition chamber and measured with a J.A. Woollam M-2000D, variable-angle, spectroscopic ellipsometer (J.A. Woollam Company, Lincoln, ME, USA) over the wavelength range of 190-1688 nm. This initial measurement provided a baseline for determining the initial thicknesses of the layers. Ellipsometric reflectance data was analyzed using the CompleteEASE® software provided by the J.A. Woollam Company. The model used for analyzing the data in CompleteEASE® is based on the layers seen in the Fig. 3.

There were three dielectrics layers that we created models for: Si_3N_4, Al_2O_3, and AlF_3. Layer 2 is CVD Si_3N_4. It is amorphous, not crystalline, and thus possesses different optical constants than the crystalline material. We had previously found that the optical constants of

Si_3N_4 could be parameterized successfully as a Tauc-Lorentz oscillator plus a Gaussian oscillator located near the band edge [4]. The same study showed that there was a thin SiO_2 layer on the surface of the Si_3N_4. Its thickness was between 1 and 2 nm, so we fixed the thickness of layer 1 at 1 nm in our model.

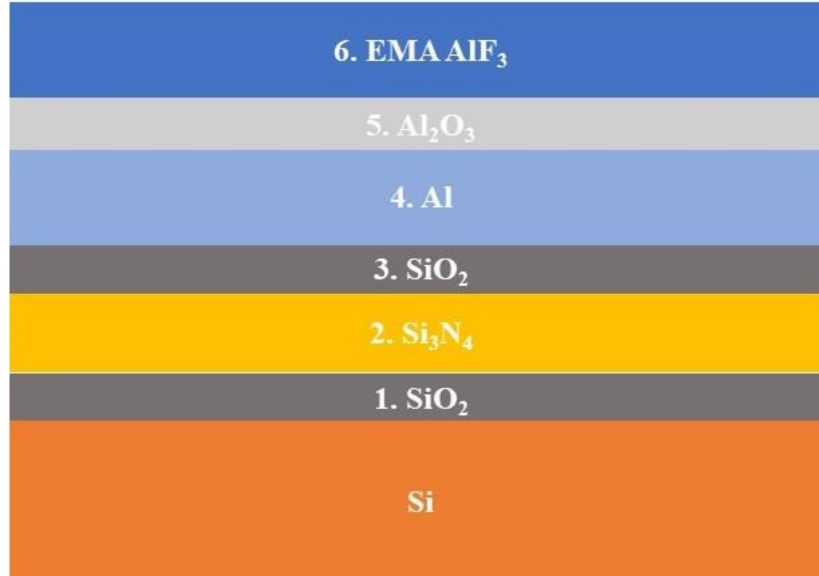

FIG. 3. Representation of the optical stack of the samples created. Layer 6 is the AlF_3 capping layer and is modeled with an effective medium approximation (EMA). Modeling layer 6 with an EMA allows us to include secondary constituents like voids and water in a primary matrix of AlF_3. Layer thicknesses are not shown to scale.

Layer 5 is the second dielectric, Al_2O_3. It is the thinnest of the layers since it is not deposited but grows from the oxidation of the Al layer. Al_2O_3 was parameterized as a Cauchy layer, with parameters fit using the CompleteEASE® software on ellipsometric data taken from the four samples that we deposited. Layer 6 is the deposited AlF_3 capping layer. As the samples aged, we observed that the fluoride layers can appear to change in apparent thickness and optical constants. One way to make sense of this observation is to model this top dielectric layer as a porous AlF_3 with bulk-like constants. The pores in the AlF_3 layer could be filled with water as water could condense from the air into the pores via capillary action. Thus, the AlF_3 layer was

modeled by using a Bruggeman effective medium approximation (EMA) layer[2], with the primary material being AlF_3 and the secondary components being void and water. We considered the void and water to be the secondary constituents in the primary AlF_3 matrix because of the porosity and solubility of AlF_3. The evaporated AlF_3 optical constants had been measured previously and were fit using a Sellmeier[3] model. This material was then used in the EMA layer for the samples deposited at room temperature. Another AlF_3 Sellmeier model with different fit parameters was used in the EMA layer for samples deposited on the heater, as it is known in the case of some fluorides the optical constants more closely resemble the bulk constants [5].

Thin film metal layers like the Al in layer 4 need to be treated differently than dielectrics because of their free electrons. The Al layer was modeled as the sum of four Gaussian oscillators with a UV pole. UV poles are Lorentz oscillators with zero broadening that remain outside the spectral range being fit.[4] The parameters of the Gaussian oscillators were fit from a previous sample of Al coated Si/Si_3N_4 wafer. The oscillator at zero eV corresponds to the free electron (Drude) contribution to Al's conductivity. The intensity and breadth of this oscillator varies with the thickness of the film and deposition conditions such as impurity concentration. We used the same Al model for each sample, not adjusting the parameters values even as the sample aged. However, it was recognized that, like the fluoride protective layer, an EMA layer could be helpful to understand aging. The aluminum would have grain boundaries and oxygen could penetrate, oxidizing the interior of the layer. Thus, we investigated this as well by inserting an

---

[2] Bruggeman EMA is the term used in the CompleteEASE® manual. It is an EMA layer where the host (primary) material is chosen, in this case, AlF_3. See CompleteEASE® user manual 9-287 for more information. The manual can be accessed online or through contact through J.A. Woollam at www.jawoollam.com.

[3] The Sellmeier layer is used to model dielectrics that accounts for UV and IR absorption. See CompleteEASE® manual 9-290 for more information.

[4] For more information on UV poles and the CompleteEASE® oscillator models, see the CompleteEASE® manual 10-332.

EMA layer composed of Al with voids and oxygen impurities. However, fitting the data in this way showed no significant evidence of voids or oxides. As a result, in our final fits to the ellipsometric data we did not characterize layer 4 as an EMA layer.

Multiple sample analysis (MSA) allows for the fitting of specified parameters for individual samples in a data set or fitting the same parameters uniformly as one value across the whole data set. It is an effective tool for finding trends that span across similar samples that would be harder to see if each set were to be analyzed sample by sample. MSA was used on present and past samples to better determine the layer optical constants of Al and AlF_3 since the optical qualities of the layers are dependent, in part, on how the samples were deposited. When fitting for the AlF_3 layer, MSA was used to best approximate the optical constants of both room-temperature deposited and heated-substrate deposited ~30 nm AlF_3 using a parametric Sellmeier model provided in the CompleteEASE® software. The two Sellmeier models were then averaged to produce reasonable constants for AlF_3 that could be used in our fitting of the ellipsometric data.

All layer thicknesses were fit excluding the SiO_2 in layer 1 and the Si substrate. Optical constants for Si and SiO_2 were provided in the CompleteEASE® software and no additional changes were made to their constants. Periodically, the samples were taken out, measured, and the ellipsometric data was saved. Our optical model, with all the layers and their parameters as discussed above, then allowed us to determine the apparent thicknesses of the films. These values were then tabulated so that we could monitor changes and identify trends in the data as they occurred.

2.2.2 Characterization via AFM

To obtain surface roughness, the samples were measured using atomic force microscopy (AFM). A 10 by 10 micron area was selected on each sample and then scanned three times. The three scans for each sample were then averaged, which resulted in a reliable capping layer roughness for each sample. It was noted that in comparing the samples, there was no significant variation in roughness between the capping layers of different samples. With these measurements we were able to fix the roughness for each sample, which helped to reduce the number of fit parameters in our ellipsometric model. Table 1 below shows the initial apparent thicknesses for each sample.

Sample	Room Temperature (RT) Substrate 1	Room Temperature (RT) Substrate 2	Heater Temperature (HT) Substrate 1	Heater Temperature (HT) Substrate 2
Roughness	2.00	1.86	1.88	2.21
6. EMA AlF_3	26.78	31.25	29.31	26.84
5. Al_2O_3	0.09	0.09	0.05	0.11
4. Al	19.9	19.9	23.6	23.1
2. Si_3N_4	306.35	304.8	301.1	298.1

TABLE 1. The initial apparent layer thicknesses measured after deposition for each of the four samples. All values in the table are in nanometers. The numbers of each row and color coordinate with Fig. 3.

2.3 Storage in 327 K Oven

After initial reflectance measurements on the ellipsometer, the samples were placed in an oven at 327 ± 10 K to simulate a hot storage room. We used a Hti© model HT 350 Temperature and Humidity Instrument® to measure the dew point and relative humidity in the oven. The dew

point of the air was 276 K and the relative humidity was 26.9%, but no attempt was made to control the humidity or dew point. Samples were taken out periodically, measured via ellipsometry and in some cases AFM, then returned to the oven over the course of about 2500 hours. The average time for removing, measuring, and returning the samples to the oven was an hour. There were also several brief power outages that resulted in the oven cooling, but it was turned on again as soon as possible.

3 Results and Discussion

3.1 Initial fit before layer parameter optimization

Many of the initial layer parameters used in the first fit were based off the CompleteEASE® data and the rest were created and fit from previous samples as discussed in Chapter 2. The first fit of the EMA AlF_3 layer is shown below in Fig. 4. Looking at Fig. 4 led us to initially think that there was significant growth in the capping layer as the time in the oven increased. However, upon reviewing the different percent values of the secondary constituents, we realized that changes needed to be made in our fitting model.

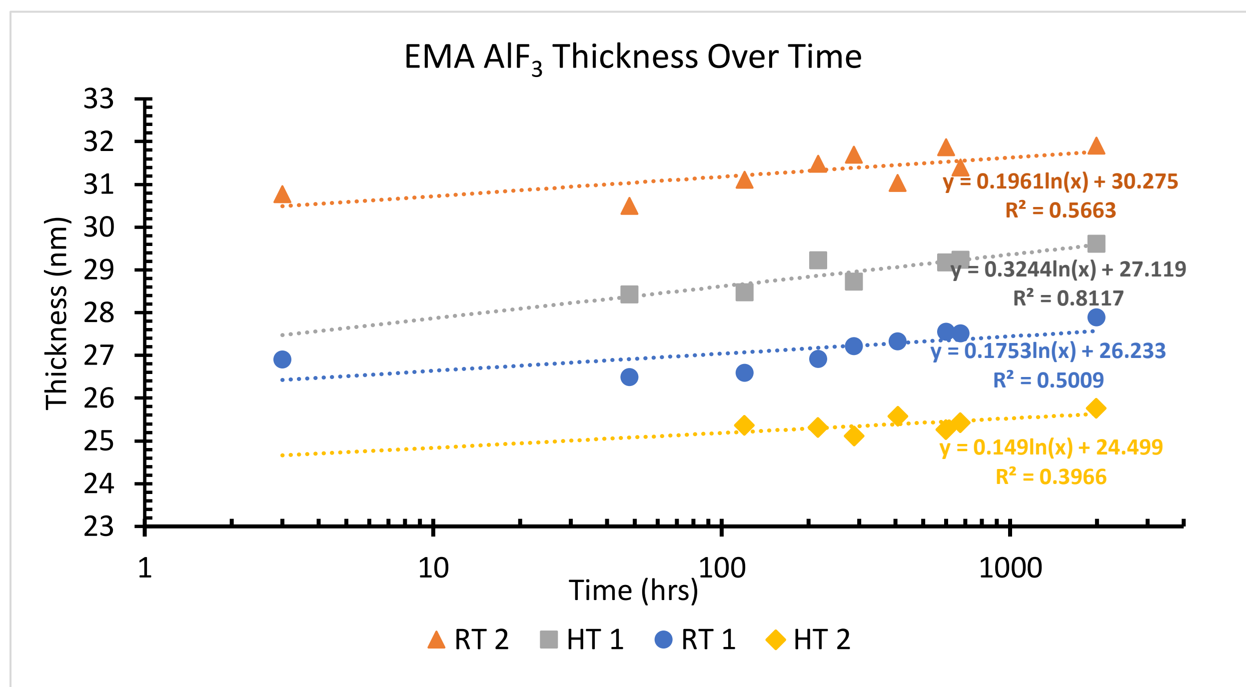

FIG. 4. The initial fit and the trends of each of the samples' AlF_3 layer over the duration in the oven. HT denotes the two samples deposited on the heater, while RT denotes the two samples that were deposited on a room temperature substrate. Note that there appears to be logarithmic growth for the AlF_3 in most samples with varying R^2 values.

3.2 Difficulties with the EMA model

3.2.1 Water as a secondary constituent

As discussed before, we thought the best model for the protective AlF_3 was an EMA layer with AlF_3 as the primary constituent and void and water as the secondary constituents. Figure 4 above shows that according to this model, each of the samples' AlF_3 thicknesses gradually increased over time. Figure 5 shows the water percentage in the AlF_3, in which all the samples started from zero and gradually increased to the 20-30% range. We doubted the high percentage of water constituent because it implies that the initial amount of AlF_3 decreased by the same amount that the water percentage increased. To figure out if the amount of water in the layer was correct, one hot sample and one cold sample were placed on a heater and held under high vacuum for 3 days. If the model was correct, then the water should have evaporated while the sample was under vacuum. After measuring the two samples immediately after removal from the heater, the data showed that the "water" percentage did not change, suggesting that the model was incorrect. Thus, we removed the "water" as a secondary constituent but kept the void as a secondary constituent that we fit over time.

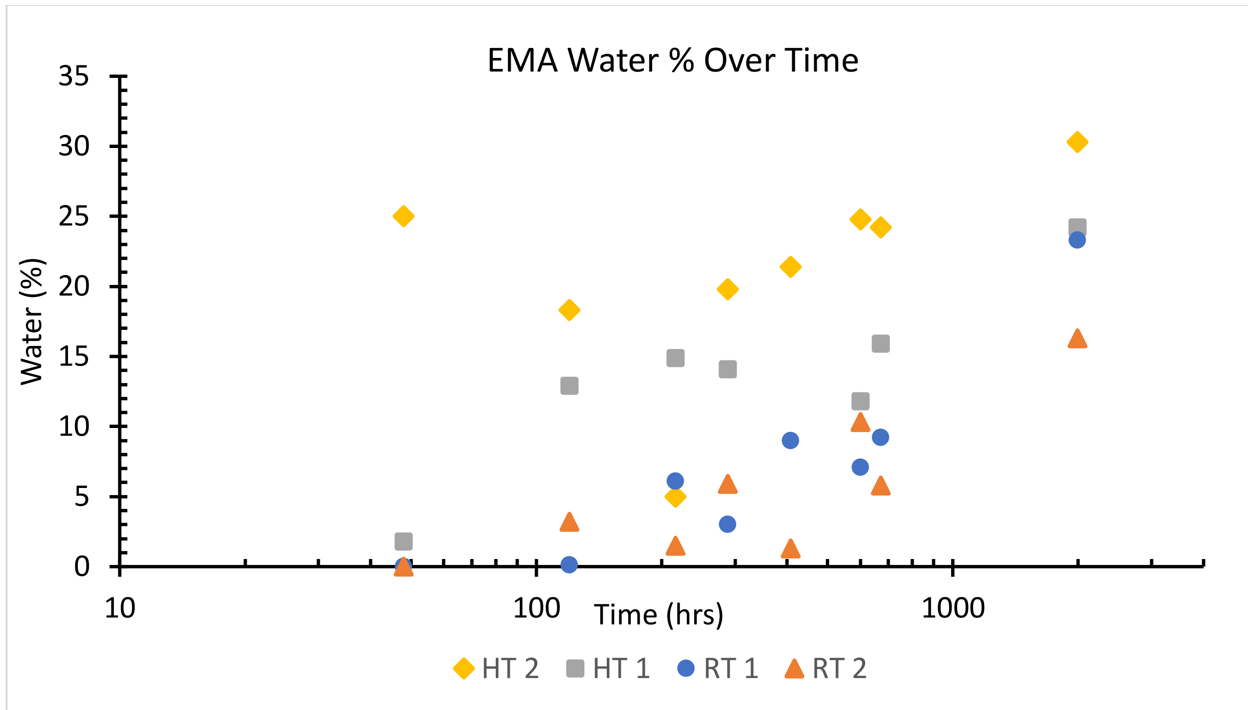

FIG. 5. The constituent "water" percent for the samples over time. If these values accurately described the state of the samples, then there would have been a significant loss of AlF_3 within the EMA layer. Notice how all samples have an increasing "water" percentage over time.

3.2.2 Void as a secondary constituent

In the initial fitting, we assumed that AlF_3 would have voids in the layer as resistive evaporation does not guarantee completely dense layers. When fitting the void constituent for the EMA AlF_3 layer, we noted that there was a significant void percentage for each sample. As time progressed, the void percentage was seen to decrease as seen in Fig. 6. We first hypothesized that this void was being filled with water, but we ruled this out as discussed in the above subsection. Despite setting the water percentage to zero and no longer fitting it, the apparent void percentage still decreased over time. This trend impelled us to better optimize all our layer parameters to see if we could determine what the voids were being filled with.

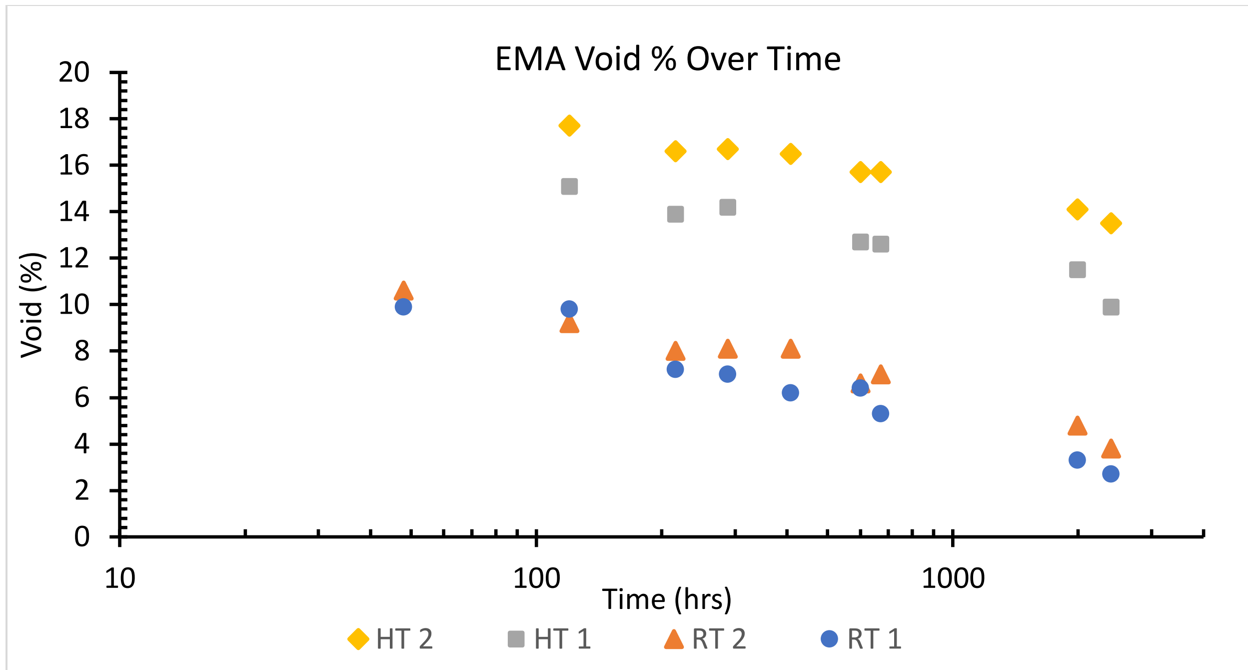

FIG. 5. Void percentage of the samples over time. Note that each sample's void percentage decreases over time. This suggests that something may be filling the voids as time progresses.

3.3 Final fit after layer parameter optimization

Seeing the void percentage trending downward led us to seek better fit parameters for the oxide layers. The first parameters we used were directly from the CompleteEASE® software. We felt that the parameters provided in CompleteEASE® software for Al_2O_3 could have been inappropriate for our alumina and we decided to replace it. As a substitute, we chose alumina since it has a similar chemical composition and is just as probable as Al_2O_3 to be in the layer stack. Incorporating the appropriate alumina was the last necessary change that we adjusted for the final fit. The fitting parameters for all other layers are discussed in depth in Chapter 2 and were kept for the final fit. Figure 7 shows the final fit of the AlF_3 layer for all samples. All samples showed no significant change in the thickness of the capping layers over the 2500 hours and two of four samples were best fit as a constant.

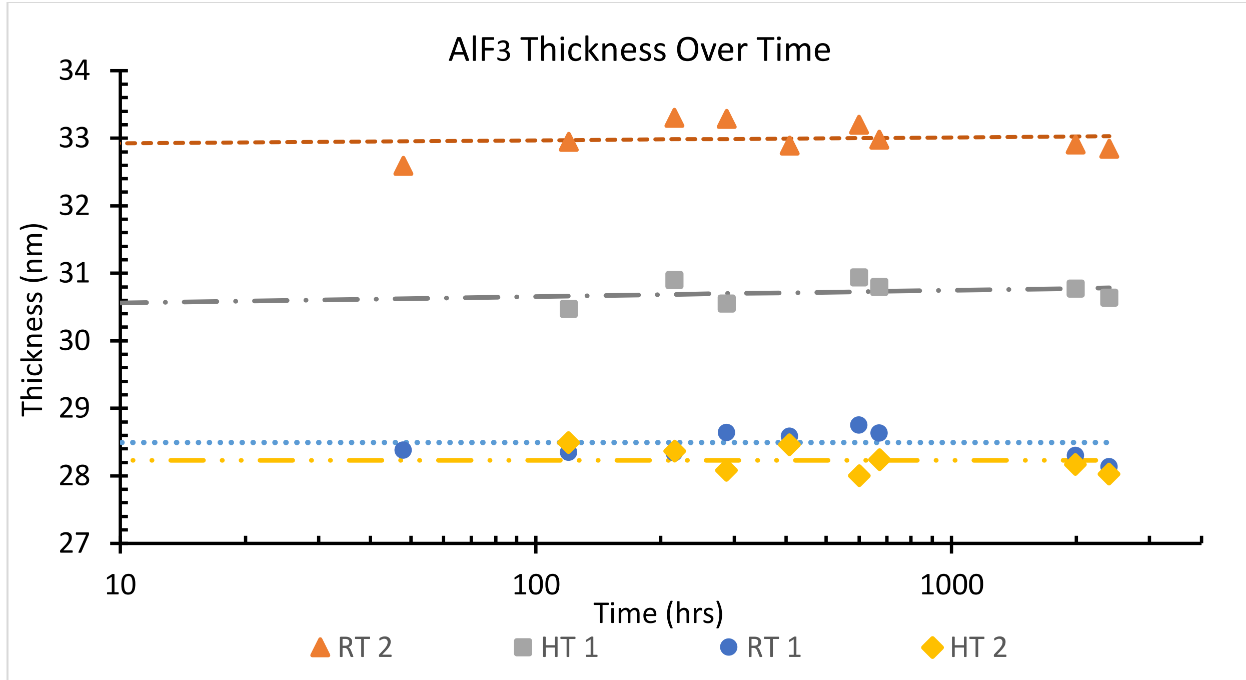

FIG. 6. The final fits of the AlF_3 capping layers for all four samples. RT denotes the two samples that were deposited on a room temperature substrate whereas HT denotes the other two samples that were deposited on a heated substrate. The logarithmic fits for each data set and the corresponding standard deviations are listed in Table 2.

TABLE 2. Best Logarithmic Fit Equations for Fig. 7

Sample	Best Logarithmic Fit	Standard Deviation (σ)
RT 1	$y = 28.49$	0.214
RT 2	$y = 0.0193\ln(t) + 32.88$	0.206
HT 1	$y = 0.0407\ln(t) + 30.47$	0.158
HT 2	$y = 28.23$	0.18

TABLE 2. All samples from the final data set for each sample were fit to $y = Aln(t) + B$ where t is measured in hours. Notice that both RT 1 and HT 1 fit the coefficient A to zero, making the logarithmic fit a constant.

3.4 Root Mean Squared Error

The primary means by which we measured the error between the data and our model was by using root mean squared errors (RMSE). With the CompleteEASE® software, a RMSE is

provided with every analyzed data set. In short, the RMSE sums the differences between the measured data and model generated data over the wavelength range[5]. An ideal model fit according to the equation used in CompleteEASE® is around 1. Figure 8 below shows the RMSEs for each data point for all four samples throughout the duration of their time in the oven. There appears to be no significant trend in the RMSEs over time, which means that our model was consistent in predicting the experimental data throughout the study. Averages of the RMSE for each sample over the duration hover around 3, which shows that our theoretical model had a good fit to the experimental data. Multilayer thin-film stacks like the ones in this study are difficult to model and an RSME near 3 is not uncommon. However, in the future we look to lower the RMSE by creating more accurate models and better understanding the aging processes in the layers.

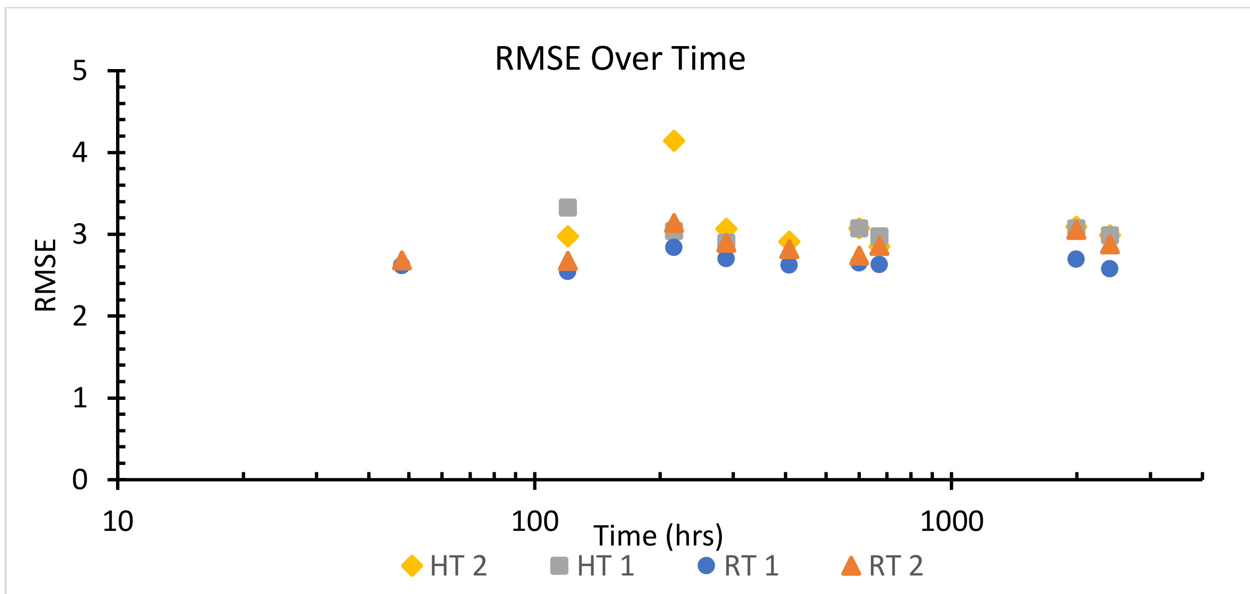

FIG. 7. The RMSE between the ellipsometric data and our model for each sample. Each data point represents the overall RMSE of the CompleteEASE® model fit to the experimental data. All data points were then plotted to determine whether or not there was a trend in the RMSEs over time, but there was no significant change in the RMSEs over time.

[5] For more information about the RMSE and how CompleteEASE® calculates it, refer to the CompleteEASE® manual page 3-49.

3.5 Conclusion

Over the course of the 2500 hours in this study, there were no significant changes in the protective AlF_3 layer while being stored in a 327 K environment, as seen in Fig. 7 above. The samples studied were analyzed using various models and layer parameters in the CompleteEASE® until an RMSE approaching 3 was achieved. In the end, the most effective model for determining the change in the AlF_3 capping layer was an EMA layer with AlF_3 as the primary matrix and voids as a secondary constituent. Initial void percentages that the model predicted for each sample were roughly halved by the end of the 2500 hours. The disappearing void percentage suggests that there is a reaction or an introduction of another substance with similar optical constants in the AlF_3 layer that was not fully accounted for. Initially it was thought that the AlF_3 was absorbing water and that accounted for the small swelling, but this idea was ruled out when the layer constants of Al and AlF_3 were optimized. In order to further understand the decrease in void percentage, other methods are needed to narrow down possible explanations that could be responsible for this observed change.

References

[1] David D. Allred, R. Steven Turley, Stephanie M. Thomas, Spencer G. Willett, Michael J. Greenburg, Spencer B. Perry, "Adding EUV reflectance to aluminum-coated mirrors for space-based observation," Proc. SPIE 10398, UV/Optical/IR Space Telescopes and Instruments: Innovative Technologies and Concepts VIII, 103980Y (5 September 2017); https://doi.org/10.1117/12.2274694

[2] Luis Rodríguez-de Marcos, Nuria Gutiérrez-Luna, Lucía Espinosa-Yáñez, Carlos Honrado-Benítez, José Chavero-Royán, Belén Perea-Abarca, Juan I. Larruquert, "Enhanced far-UV reflectance of Al mirrors protected with hot-deposited MgF2," Proc. SPIE 10691, Advances in Optical Thin Films VI, 106910T (5 June 2018); https://doi.org/10.1117/12.2313635

[3] Hennessy, J., Jewell, A.D., Balasubramanian, K., Nikzad, S., 2016. Ultraviolet optical properties of aluminum fluoride thin films deposited by atomic layer deposition. Journal of Vacuum Science & Technology A 34, 01A120.. doi:10.1116/1.4935450

[4] C.V. Cushman, B.I. Johnson, A. Martin, B.M. Lunt, N.J. Smith, and M.R. Linford, Surface Science Spectra **24**, 026001 (2017).

[5] Véronique Dauer, "Optical constants of lithium fluoride thin films in the far ultraviolet," J. Opt. Soc. Am. B 17, 300-303 (2000)

Index

A

AFM · 12

E

effective medium approximation · 8
Ellipsometry · 7

M

Multiple sample analysis · 10

R

RMSE · 17

S

Sellmeier · 9